

Cancer Heterogeneity and Imaging

James P B O'Connor^{1,2}

¹ Institute of Cancer Sciences, University of Manchester, Manchester, UK

² Department of Radiology, The Christie Hospital NHS Trust, Manchester, UK

ABSTRACT

There is interest in identifying and quantifying tumor heterogeneity at the genomic, tissue pathology and clinical imaging scales, as this may help better understand tumor biology and may yield useful biomarkers for guiding therapy-based decision making. This review focuses on the role and value of using x-ray, CT, MRI and PET based imaging methods that identify, measure and map tumor heterogeneity. In particular we highlight the potential value of these techniques and the key challenges required to validate and qualify these biomarkers for clinical use.

INTRODUCTION

Tumors are biologically heterogeneous (1, 2). This fact has been the subject of much interest following recent high profile studies that have begun to map and track the presence of genetic variation in tumors. These findings have started to investigate the relevance that these findings may have for the treatment of patients with cancer (3). Spatial variation in cell genetic profiles leads to altered microenvironments. This regional variation is visible through analysis of tissue pathology images (4). The current understanding of cancer heterogeneity from the perspectives of genomics and tissue pathology are covered elsewhere in this special issue.

In this article, we focus on the role and value of using imaging methods to identify, measure and map the tumor heterogeneity that arises from genetic and tissue pathology variation and can be identified using imaging techniques. Particular emphasis is placed on clinically available imaging techniques such as x-ray computed tomography (CT), magnetic resonance imaging (MRI) and positron emission tomography (PET) that are readily available and enable the non-invasive whole-lesion sampling of tumor structure and function (5, 6).

TERMINOLOGY

Different research studies describe different conceptual types of tumor spatial heterogeneity. The variation in structure and function found between different tumors in individual patients is termed intertumor heterogeneity. In distinction, the spatial variation seen within individual lesions is termed intratumor heterogeneity. Finally, some studies compare the differences in lesions between different patients, termed interpatient heterogeneity. Imaging methods can be used to study all three of these scenarios. In this article, we focus on intratumor heterogeneity, assessed by regarding tumors as 3D structures composed of individual 3D pixels known as voxels.

While much of the terminology used in imaging studies of tumor heterogeneity are similar or identical to the terms used in genomic and tissue pathology research, it is important to appreciate that clinical imaging is performed on a different scale. This has important sequelae, and there is considerable need for investigators to determine how these different insights into tumor biology can be combined into models that describe disease optimally. Although several genomic studies of heterogeneity have achieved high profile status, it is important to remember that extensive genomic profiling of tumors is still only performed on a sub-set of patients' tumors, whereas image-based whole tumor sampling is performed

repeatedly during diagnosis, staging and response assessment in nearly all patients with solid tumors (7).

CURRENT CLINICAL USE OF IMAGING DATA

Clinical imaging has been recognized as one of the great advances in modern medicine (8). It has revolutionized how oncologists diagnose and stage solid tumors, by detecting the presence of a cancer and by mapping the locations of the primary lesion and its metastases (9). Imaging is also central to assessing response to therapy and in detecting disease recurrence, by measuring change in lesion size (10) and (sometimes) lesion function (11). Imaging is used to identify patients at risk of toxicity (for example, cardiotoxicity may preclude use of some chemotherapy agents) (12). Finally, imaging can detect complications from the cancer (for example urinary tract obstruction) and the treatments (for example, presence of lung consolidation due to pneumonia) (13).

For the above applications, tumor heterogeneity is not generally considered a key consideration. However, for some indications, radiologists interpret spatial heterogeneity in clinical images on a daily basis. The fact that many breast lesions are spiculated has been recognised for many decades, and this feature forms part of the BI-RADS classification for evaluating risk of malignancy (14, 15), with spiculation indicating a very high risk of a mass being malignant (Figure 1a). In another example, tumors are composed often of different regions including highly vascular and avidly enhancing regions, enhancing soft tissue and relatively non-enhancing regions, which include areas of necrosis within the tumor as well as haemorrhage. Some tumours, for example high grade glioma, also have areas of surrounding edema. These features can be appreciated readily using sequences that identify tumor anatomy and morphology, along with some functional information (here, enhancement due to administration of intravenous contrast agents; Figure 1b). In addition, other imaging techniques, such as ^{18}F FDG PET-CT provide functional information, such as metabolic activity, and these techniques can also be used to identify regional variation in tumor function in solid tumors (Figure 1c) (11). It is important to appreciate that in these examples, spatial heterogeneity tends to be reported using qualitative description (e.g. ‘enhancing rim versus non-enhancing core’, or ‘focal region of intense tracer avidity’).

There has been considerable effort over the last decade to convert these qualitative observations of heterogeneity into quantitative *biomarkers* for clinical use. A biomarker is a “defined characteristic that is measured as an indicator of normal biological processes, pathogenic processes or responses to an exposure or intervention, including therapeutic

interventions” (16, 17). An imaging biomarker is a measurement derived from one or more medical images (18). This idea represents an important paradigm shift, where images are regarded as being composed of arrays of data, arranged spatially in individual 3D voxels (7). Here, each individual voxel is a cube (or cuboid) of data which summarizes a particular morphologic, metabolic or physiologic signal over a volume of around $(0.25 - 5)^3$ millimetres, depending on modality and subject (animal or human).

CONSIDERATIONS FOR VOXEL-WISE ANALYSIS OF CLINICAL IMAGES

Several important factors must be considered when analyzing images on a voxel-wise basis. Firstly, some voxels suffer partial volume averaging (typically at interface with non-tumor tissue), so may only partially represent tumor tissue. Secondly, there is inevitable compromise between having sufficient numbers of voxels to perform the analysis versus sufficiently large voxels to overcome noise and keep imaging times practical (19). Most analysis methods require hundreds to thousands of voxels for robust application.

Thirdly, many clinical studies of tumor spatial heterogeneity have used imaging protocols determined by healthcare considerations, rather than optimizing research needs; for example, portions of tumor will be omitted when non-contiguous tumor sampling is used (20) which confounds 3D spatial analyses (21). Fourthly, some calculated voxel values, such as apparent diffusion coefficient (ADC), contrast transfer coefficient (K^{trans}) and blood flow are derived from multiple images obtained over time. Optimal estimation of the errors associated with motion will vary for different parameters and for different voxels. This issue is seldom considered when assessing intratumor heterogeneity (22).

STRATEGIES FOR IMAGING INTRATUMOR SPATIAL HETEROGENEITY

Nearly all malignant tumors show intratumor heterogeneity on imaging, although the extent varies between pre-clinical cancer models and between patients (23). Spatial variation is dynamic, for example, variations in tumor pO_2 can be mapped and have been shown to fluctuate over minutes to hours using a range of imaging techniques (24, 25). Furthermore, the degree of intratumor heterogeneity tends to increase as tumors grow (26, 27).

There is considerable research interest in identifying and measuring both the overall degree of spatial tumor heterogeneity and also which sub-populations within tumors are responsible for mediating response to therapy and resistance (28). The clinical significance of

established spatial heterogeneity is discussed in detail elsewhere in this special issue, but in general, greater heterogeneity tends to indicate a relatively poor clinical outcome (29). This is considered, in part to result from resistant subpopulations of cells driving resistance to therapy (5, 30). However, it is important to note also that the extent and visualised patterns of intratumor heterogeneity may either increase or decrease following efficacious anti-cancer therapy (31, 32), depending on lesion type, imaging modality and choice of therapy.

There are three distinct families of approach used to derive quantitative biomarkers of intratumor heterogeneity. It is important to appreciate that the same image data can be used to measure conventional clinical parameters (e.g. size), functional parameters that describe pathophysiological correlates in the tumor (e.g. average blood flow and permeability) and also the various different heterogeneity based metric that are detailed below (Figure 2). All of these parameters can be considered biomarkers.

Defining tumor sub-regions

Perhaps the most obvious approach to quantify intratumor heterogeneity attempts to identify the geographic sub-regions that drive response to therapy, subsequent resistance and relapse during treatment failure (5). This idea reflects the fact the tumor tissue is composed of regional habitats with discrete tumor biology (7). In order to define sub-regions, decisions must be made to enable identification of individual voxels with common structural or biological features. In general, tumor images contain hundreds-thousands of voxels, so 'similar' voxels must be grouped together (parcellation). This can be performed using various techniques with differing underlying assumptions and methodology. It is important to recognize that some imaging signals from neighboring voxels are not necessarily entirely independent, as seen in advanced MRI techniques where zero-filling techniques are employed to keep scan times as fast as allowable (33) and so this must be controlled for when defining sub-regions.

Data-driven voxel classification methods

One common approach is to use a data-driven clustering approach such as Gaussian mixed-models or k-means clustering and then applying a principal components analysis (34). Here, multiple imaging parameters (for example K^{trans} and ADC derived from MRI) can be used to group voxels with similar signals (or 'spectra') into functionally coherent regions within a lesion (35). Most multi-spectral analyses use pattern recognition techniques that analyze images to identify voxel clusters in a multi-dimensional feature space. A classifier then groups individual voxels together based on their similarities and differences (36).

Unfortunately, considerable statistical challenges are associated with generating regional voxel groupings in normal structures (e.g. brain) in a technically valid fashion. This challenge has added complexity in heterogeneous structures, such as tumors, where predictable voxel patterns are lacking (37). Further difficulties are encountered when attempts are made to use segmentation to track tumors in time, since lesions change shape and volume as tumors grow, respond to therapy and relapse (22). Investigators must either use non-rigid registration methods, to establish the best approximate voxel correspondence, accepting that this problem is inherently limited, or must simplify their understanding of tumor growth and shape change (38).

Imposed voxel classification methods

An alternative approach – with a similar aim to data-driven methods, of grouping together voxels with similar underlying biology – is to define voxels by binary features (e.g. presence or absence signal enhancement) or by applying a threshold to a continuous variable feature (e.g. magnitude value of (^{18}F -FDG PET SUV_{max} or K^{trans}) (22). Here, a decision is made, with underlying assumptions, as to the categorization having a meaningful relationship to biology and to clinical outcome.

It is important to realize that these simple approaches have several caveats. Firstly 'binary' features such as enhancement are not absolute. Instead, they depend critically on how images are acquired and analyzed. In DCE-CT and DCE-MRI data, for example, enhancement could be defined as having an area under the contrast agent concentration-time curve greater than zero (where > 0 defines positive enhancement) or could be defined by comparing pre- and post- enhancement time points using a statistical test (where $p < 0.05$ defines negative or positive enhancement on a two sided t-test) (39, 40). Alternatively enhancement-weighted analyses may be performed (41). Secondly, threshold values for continuous data based on 'cut points' selected to enhance statistical separation in studies are often arbitrary and may have biological basis (19).

Imposed geographic methods

Tumor regions may be defined geographically, for example by modeling tumors as spheres with concentric radial sub-regions (42) or by labelling voxels as 'rim' or 'core' based on relative voxel position in histogram distributions (43). In these approaches a priori assumptions are imposed on tumors concerning their macroscopic structure. This approach may have some use in reproducible preclinical models of tumors, but is generally seen as a non-realistic model for clinical tumours.

Example application: imaging sub-region hypoxic signatures

Most solid tumors contain hypoxic sub-regions and greater hypoxic fractions are considered a poor prognostic indicator (44). There are several reasons why imaging hypoxia may be useful for clinicians. Firstly, there is current interest in using imaging to 'dose paint' the radiotherapy dose administered to each individual tumor, based on the spatial characteristics detected. Initial interest here has been on using ^{18}F FDG PET data (45). This concept is based on different sub-regions being relatively radio-resistant (46) and recurrent disease arising in areas with greatest metabolic abnormality (47). Since subsequent work has shown that the interplay between abnormal metabolic, vascular and hypoxic expression in tumors may vary in an unpredictable manner (48), there is a strong rationale to investigate whether hypoxic regions should be treated with differing doses to well-oxygenated tumor.

Secondly, imaging is one strategy under investigation – along with gene based approaches (49) – to stratify patients for treatment, based on measuring pre-treatment hypoxic status (50). Several targeted therapies have been developed that purport to improve tumor oxygenation, to improve prognosis and response to therapies including radiotherapy. Unfortunately, results at phase III have been disappointing, with little survival benefit being reported in patients treated by the targeted therapy in combination with conventional radiation-based treatment (51). For example, the hypoxia activated prodrug evofosfamide (TH-302; Threshold Pharmaceuticals, Inc., CA) was reported recently to provide no overall survival benefit in two phase III studies in patients with advanced pancreatic cancer and advanced soft tissue sarcoma, despite promising pre-clinical data (52). No patient selection was performed for these studies despite preclinical data that TH-302 monotherapy or in combination with radiotherapy provided significant growth delay in sarcoma and lung models of cancer, mediated by reduction in hypoxic fraction (53). This suggests strongly that trial design with patient selection – identifying which patients had significant hypoxia that could be modified – may have been able to demonstrate clinical utility.

Thirdly, while there is great interest in identifying pre-treatment hypoxic status, there is some preliminary evidence that early preservation of hypoxia predicts treatment failure. In a pilot study of patients with head and neck cancer treated with chemoradiotherapy, the degree of reduction in hypoxia at 1 or 2 weeks during treatment, detected by FMISO PET imaging, appeared to identify patients that might benefit from hypoxia modification or dose-escalated treatment (54). Imaging enables these changes to be identified, quantified and mapped.

Both PET and MRI based techniques enable a non-invasive 3D sampling of the extent of tumor oxygenation levels to distinguish hypoxic and normoxic sub-regions from one another (55, 56). Several PET based methods have been used in preclinical and clinical

investigations, but most current studies use ^{18}F based techniques, including FMISO, FAZA and HX4 (57). These tracers have differences in their radiotracer properties such as onset and duration of tumor to background ratio, as well as factors such as spatial reproducibility and sensitivity to oxygen modulation (58). Further work is required to determine if one tracer is superior or if decisions can be made due to local preference. Initial clinical data suggest that these methods can provide spatially stable signals in patients, for example, for HX4 data showing 15-17% co-efficient of variation on two examinations prior to therapy in patients with head and neck or lung cancer (59), although discrepant findings have been observed in some patients in other studies (60). Initial clinical studies have provided preliminary evidence that FMISO detected early preservation of hypoxia predicts treatment failure from chemoradiotherapy in patients with head and neck cancer (54) and that tumor recurrence may occur within the hypoxic sub-regions identified by FMISO imaging (61).

In MRI, methods such as blood oxygenation level dependent imaging (62) have failed to translate into widespread clinical use; DCE-MRI has been used in several studies (63) but at best the derived biomarkers (e.g. blood flow) have an indirect relationship to hypoxia (64). Recently, we and others have developed a novel method of using oxygen-inhalation to unmask which tumor sub regions are hypoxic, termed oxygen-enhanced MRI (65, 66). This method has potential to non-invasively map regional hypoxia with higher spatial resolution than PET techniques (56). Although this technique is less well established than PET based methods, it has already been shown feasible and tolerable in patients with a variety of solid tumors (67, 68). There is emerging evidence that oxygen-enhanced MRI can detect signal changes that correspond spatially and temporally with the evolution of hypoxia, as measured by pimonidazole adduct formation (65, 66) (Figure 3). As with data from PET based methods (53), the technique appears sensitive to dynamic flux in pO_2 (66). Encouragingly, there is also initial evidence that oxygen-enhanced MRI may predict response to radiotherapy (69).

Quantifying the overall spatial complexity of tumors

Tumors can be regarded as objects of varying spatial complexity. This complexity – a feature dependent on the heterogeneity present in the object – can be quantified as used as a biomarker. Various forms of feature analysis have been used.

Texture analysis

There is a long standing history of using computer aided detection (CAD) systems to classify tumors by feature analysis, particularly in studying breast cancer risk (70). In texture analysis, several similar approaches can be used, for example the Haralick method (71) where a co-occurrence matrix element denoted $P_{d,\theta}(i, j)$ measures the probability of starting

from any image voxel with designated value i , moving d voxels along the image in direction θ , and then arriving at another voxel with value j . The resultant co-occurrence matrix is a 2D histogram which describes a joint distribution of all the possible moves with step size d and direction θ on the image. Many features can be extracted from this matrix, including measurements of lesion contrast, shape and spatial complexity.

Fractal analysis and Minkowski functionals

Fractal dimensions estimate the complexity of geometrical patterns which result from abstract recursive procedures (72). The simplest fractal dimension is the box-counting dimension (d_0). This is calculated by imposing regular grids of a range of scales on a binary object, such as a tumor, and then counting the number of grid elements (boxes) that are occupied by the object at each scale. The parameter d_0 is the slope of the line of best fit when plotting the number of occupied boxes against the reciprocal of the scale on log-log axes (73) (Figure 4a). Increasingly complex variants can incorporate continuous scale values of parameters such as ADC magnitude value. Minkowski functionals analyse binarized images over a range of thresholds and also quantify space-filling properties of tumors.

Example application: single parameters

Traditionally, most feature analyses have derived the putative biomarkers using in-house software. This makes comparison of the data published by different groups difficult, since it is not always clear exactly how different feature-based biomarkers relate to one another. In some cases – such as with CAD in breast cancer – there are software tools approved for use by FDA and other regulators (74) and so these feature-based biomarkers have crossed the Cooksey translational gaps (75, 76) to be used in healthcare.

The potential value for feature based analysis is reviewed in depth elsewhere (77). In general one feature or a small number of features is derived. Typical applications have distinguished malignant lesions from benign lesions, in various cancer types including early stage cancers of the colon (78) and the lung (79). Similar methods have distinguished low and high grade glioma tumors from one another (80). Texture based methods can also act as pharmacodynamic biomarkers of response, for example to patients with renal cancer lesions treated with tyrosine kinase inhibitors (81), and may have value as predictive biomarkers, for example in lung cancer (82).

These data are interesting and as a result several companies have begun to commercialise software tools that enable characterisation of image texture (83). However, it is unclear at

present how many derived texture, fractal, Minkowski functionals and other similar metrics relate to one another. Crucially, while these parameters show promise, they are complicated to derive, have uncertain relationship to underlying tumor biology and significant results are not necessarily of additional benefit compared to simple average value parameters derived from the same data (such as median blood flow or median SUV_{max}) (22).

Example application: Using radiomics to mine image data

Some studies have shown that extra prognostic or predictive information is contained in the feature-based parameter, above and beyond that contained in size or average value functional data. For example, in a small study of patients with colorectal cancer liver metastases, the fractal dimension d_0 increased predictive power in a multivariate model describing volume reduction following treatment with bevacizumab and with cytotoxic chemotherapy (84) (Figure 4b). This and other data provides some justification for the concept that quantifying heterogeneity enables the maximum yield from data already required in routine clinical radiological practice.

'Radiomics' is a relatively new term, which the conversion of images to higher dimensional data and the subsequent mining of these data for improved decision support. Radiomics is explicitly a process designed to extract a large number of quantitative features from digital images such as those acquired daily in cancer radiological practice. Steps are shown in Figure 4c and include image acquisition, identifying the tumor region of interest (both whole tumor and sub-regions), image segmentation, and feature extraction. Finally, these features must be entered into an appropriate searchable database and then the data is mined (7). Since radiomics is designed to develop decision support tools, mining of the feature-based image data may be combined with other patient meta-data (e.g. demographics and genomic data) to generate or test a hypothesis and to increase the power of the decision support models (85). The details and rationale for this process is described elsewhere (86).

Many of the features defined in radiomics are familiar to clinicians. These include size, shape, vascularity, necrosis, spiculation and other features and have been termed 'semantic' since they are typically described by radiologists. However, in the radiomic setting, these features are extracted with CAD to achieve higher standardization, higher inter-observer agreement and faster throughput. However, many more features extracted are mathematical descriptors that are not typically described in radiological reports, and have been termed 'agnostic' features. Examples include first order statistics (essentially histogram parameters such as median, centiles, skewness, kurtosis and entropy, that ignore spatial distribution of voxel values), second order statistics (essentially the features based on texture) and higher order statistics (essentially methods that impose filter grids on images to extract patterns,

such as fractals, Laplacian transforms and other analyses of spatial arrangement of voxel values) (7).

In a landmark study, a signature was developed in a training dataset from Maastricht of 422 patients with NSCLC. Here, 440 quantitative image features that were based on image intensity, shape, texture and multiscale wavelet were reduced to four features and then applied to three further datasets: a further 225 patients with NSCLC at Radboud, Nijmegen, and also to two studies of head and neck cancer from Maastricht (n=136) and Amsterdam (n=89). A multivariate Cox proportional hazards regression model was used to predict survival and was highly significant in all the sub-studies, indicating that the radiomic approach has prognostic significance. Importantly, the radiomic approach also outperformed size based assessment in two of the three sub-studies (87).

This study demonstrates the potential power of heterogeneity analysis using imaging. A key strength of this 'radiomic' analysis is that substantial patient data is available when using clinical CT, MRI and PET data images. Thus, unlike the above section – where the identification and characterization of tumor sub-regions generally requires the use of bespoke multi-parametric imaging protocols that presently are firmly within the research domain – radiomic analysis can profile the spatial heterogeneity of tumors and may provide significant additional information over that obtained by current imaging methods.

However, some notes of caution should be sounded. To date relatively few studies have applied this approach and there is urgent need for the radiomics method to be applied more widely in other cancer centers, to see if results are replicated. Despite the relatively small number of current studies, there is no one single 'radiomic approach'. Studies have varied from employing tens of parameters, to around 200 features (88), over 400 features (87) or over 600 features (89). The data from each of these studies are related, but cannot be seen as describing one biomarker; rather in each case the radiomic signature should be regarded as a cousin of those described in other studies. Further, while some initial studies suggest that the radiomic signatures may have positive associations with histopathologic (90) and molecular profiles (91, 92), there is great need to better understand the relationships between feature-based biomarkers and pathology readouts.

Summarising data distributions with histograms

Voxel values can be plotted as histograms, from which many simple descriptors can be extracted as potential biomarkers (93). These include simple descriptors of image

heterogeneity such as standard deviation, interquartile range, n^{th} centile(s), skew and kurtosis, as well as mean and median values (94). In these approaches the inherent spatial relationship between voxels is discarded and data are treated as a list of continuous variables.

Histograms can be generated using widely available software, so histogram analysis has proved popular method for characterizing intratumoral heterogeneity (95). Several important points should be considered. Histogram analyses have high dimensionality and generate many parameters, so require correction for multiple comparisons (96). The repeatability and reproducibility of many histogram-derived parameters are uncertain and have not yet been evaluated in multi-centre studies (19). Further, many parameters, such as 5th centile or kurtosis, have no clear biological correlate making biological validation difficult.

VALIDATION OF HETEROGENEITY BIOMARKERS

Despite their great potential, most biomarkers fail to alter clinical practice (97, 98). There is growing realization in the imaging science, radiology, cancer biology and oncology communities that imaging biomarkers must undergo more rigorous technical validation, biological/clinical validation, and qualification if they are to alter clinical decision making (18) (Figure 5). While this is an important point for imaging biomarkers in general, it is particularly apt for image-based heterogeneity biomarkers since very few of these biomarkers have undergone extensive validation or qualification.

Biomarker repeatability and reproducibility are vital to establish measurement precision (99). Simulations and phantom experiments can help establish measurement technical accuracy (100). Attention to these steps is essential early on in development and also as promising biomarkers transition into multicenter settings. For feature-based and histogram parameters, simple conventional statistical analyses may be appropriate, such as parameter co-efficient of variation. However, for spatially congruent biomarkers that quantify tumor sub-regions, it may also be appropriate to use measurements such as DICE overlap fraction (101). Finally, for radiomic analyses that generate a very large number of parameters, the analysis model must be built on test data and then applied in validation cohorts to avoid excessive multiple comparisons and the 'curse of dimensionality' (96) associated with high dimension data.

Biological validation is an important step for imaging biomarkers. However, for all imaging it should be remembered that image data is acquired on an entirely different scale from histopathology data. Typically voxel dimensions are 200-2000 μm for rodent models and

750-5000 μm for clinical tumors, so pathological sections sample only a small subset of the tissue captured by a corresponding imaging slice. While it may be appropriate to use tissue pathology to validate imaging biomarkers that quantify tumor sub-regions (e.g. necrosis, hypoxia) with pathology methods that purport to measure the same processes (102, 103), it is important to appreciate that many imaging biomarkers do not have an equivalent tissue pathology correlate, particularly feature-based and histogram-derived biomarkers (18). Even where this method is appropriate there is no consensus as to how commercial (104) or in house segmentation algorithms should analyze either the radiology or pathology images. The limits of biological validation may be circumvented where large enough datasets exist, since imaging biomarkers can be compared directly with clinical endpoints such as quality-adjusted life year, progression-free survival or overall survival (18).

CONCLUSION

Clinical imaging methods have great potential to identify, quantify and map intratumoral heterogeneity. An extensive literature exists on the theory and applications of various methods, some of which identify tumor sub-regions, whereas other methods quantify the overall spatial heterogeneity and complexity of individual lesions. However, there is need to identify clearly which unmet needs will be served by developing, validating and qualifying new imaging biomarkers of heterogeneity. Further, how these imaging biomarkers should be compared with or added to genomic, proteomic, metabolomic and tissue pathology based biomarkers of heterogeneity is at present unclear, but is an area for great potential multidisciplinary collaboration.

REFERENCES

1. Heppner GH. Tumor heterogeneity. *Cancer Res.* 1984 Jun;44(6):2259-65.
2. Bedard PL, Hansen AR, Ratain MJ, Siu LL. Tumour heterogeneity in the clinic. *Nature.* 2013 Sep 19;501(7467):355-64.
3. Burrell RA, McGranahan N, Bartek J, Swanton C. The causes and consequences of genetic heterogeneity in cancer evolution. *Nature.* 2013 Sep 19;501(7467):338-45.
4. Heindl A, Nawaz S, Yuan Y. Mapping spatial heterogeneity in the tumor microenvironment: a new era for digital pathology. *Laboratory investigation; a journal of technical methods and pathology.* 2015 Apr;95(4):377-84.
5. Gatenby RA, Grove O, Gillies RJ. Quantitative imaging in cancer evolution and ecology. *Radiology.* 2013 Oct;269(1):8-15.
6. O'Connor JP, Jackson A, Asselin MC, Buckley DL, Parker GJ, Jayson GC. Quantitative imaging biomarkers in the clinical development of targeted therapeutics: current and future perspectives. *Lancet Oncol.* 2008 Aug;9(8):766-76.
7. Gillies RJ, Kinahan PE, Hricak H. Radiomics: Images Are More than Pictures, They Are Data. *Radiology.* 2016 Feb;278(2):563-77.
8. Looking back on the millennium in medicine. *N Engl J Med.* 2000 Jan 6;342(1):42-9.
9. Edge SB, Byrd DR, Compton CC, Fritz AG, Greene FL, Trotti A. *AJCC Cancer Staging Handbook (7th edition).* 5th ed. New York: Springer; 2010.
10. Eisenhauer EA, Therasse P, Bogaerts J, Schwartz LH, Sargent D, Ford R, et al. New response evaluation criteria in solid tumours: revised RECIST guideline (version 1.1). *Eur J Cancer.* 2009 Jan;45(2):228-47.
11. Barrington SF, Mikhaeel NG, Kostakoglu L, Meignan M, Hutchings M, Mueller SP, et al. Role of imaging in the staging and response assessment of lymphoma: consensus of the International Conference on Malignant Lymphomas Imaging Working Group. *J Clin Oncol.* 2014 Sep 20;32(27):3048-58.
12. Plana JC, Galderisi M, Barac A, Ewer MS, Ky B, Scherrer-Crosbie M, et al. Expert consensus for multimodality imaging evaluation of adult patients during and after cancer therapy: a report from the American Society of Echocardiography and the European Association of Cardiovascular Imaging. *J Am Soc Echocardiogr.* 2014 Sep;27(9):911-39.
13. Husband JE, Reznick RH. *Imaging in oncology.* London: Taylor & Francis; 2004.
14. Orel SG, Kay N, Reynolds C, Sullivan DC. BI-RADS categorization as a predictor of malignancy. *Radiology.* 1999 Jun;211(3):845-50.
15. Burrell HC, Pinder SE, Wilson AR, Evans AJ, Yeoman LJ, Elston CW, et al. The positive predictive value of mammographic signs: a review of 425 non-palpable breast lesions. *Clin Radiol.* 1996 Apr;51(4):277-81.
16. Biomarkers Definitions Working Group. Biomarkers and surrogate endpoints: preferred definitions and conceptual framework. *Clin Pharmacol Ther.* 2001 Mar;69(3):89-95.
17. FDA-NIH Biomarker Working Group. BEST (Biomarkers, EndpointS, and other Tools) Resource. <http://www.ncbi.nlm.nih.gov/books/NBK326791> (accessed 4th February 2016).
18. O'Connor JPB, Aboagye EO, Adams JE, Aerts HJWL, Barrington SF, Beer AJ, et al. Imaging Biomarker Roadmap for Cancer Studies *Nat Rev Clin Oncol.* 2016;13:Accepted, In Press.
19. Jackson A, O'Connor JP, Parker GJ, Jayson GC. Imaging Tumor Vascular Heterogeneity and Angiogenesis using Dynamic Contrast-Enhanced Magnetic Resonance Imaging. *Clin Cancer Res.* 2007 Jun 15;13(12):3449-59.
20. Pope WB, Kim HJ, Huo J, Alger J, Brown MS, Gjertson D, et al. Recurrent glioblastoma multiforme: ADC histogram analysis predicts response to bevacizumab treatment. *Radiology.* 2009 Jul;252(1):182-9.
21. Chen W, Giger ML, Li H, Bick U, Newstead GM. Volumetric texture analysis of breast lesions on contrast-enhanced magnetic resonance images. *Magn Reson Med.* 2007 Sep;58(3):562-71.

22. O'Connor JP, Rose CJ, Waterton JC, Carano RA, Parker GJ, Jackson A. Imaging intratumor heterogeneity: role in therapy response, resistance, and clinical outcome. *Clin Cancer Res*. 2015 Jan 15;21(2):249-57.
23. Meacham CE, Morrison SJ. Tumour heterogeneity and cancer cell plasticity. *Nature*. 2013 Sep 19;501(7467):328-37.
24. Serganova I, Doubrovin M, Vider J, Ponomarev V, Soghomonyan S, Beresten T, et al. Molecular imaging of temporal dynamics and spatial heterogeneity of hypoxia-inducible factor-1 signal transduction activity in tumors in living mice. *Cancer Res*. 2004 Sep 1;64(17):6101-8.
25. Cardenas-Navia LI, Mace D, Richardson RA, Wilson DF, Shan S, Dewhirst MW. The pervasive presence of fluctuating oxygenation in tumors. *Cancer Res*. 2008 Jul 15;68(14):5812-9.
26. Eskey CJ, Koretsky AP, Domach MM, Jain RK. 2H-nuclear magnetic resonance imaging of tumor blood flow: spatial and temporal heterogeneity in a tissue-isolated mammary adenocarcinoma. *Cancer Res*. 1992 Nov 1;52(21):6010-9.
27. Brurberg KG, Gaustad JV, Mollatt CS, Rofstad EK. Temporal heterogeneity in blood supply in human tumor xenografts. *Neoplasia*. 2008 Jul;10(7):727-35.
28. Alizadeh AA, Aranda V, Bardelli A, Blanpain C, Bock C, Borowski C, et al. Toward understanding and exploiting tumor heterogeneity. *Nat Med*. 2015 Aug;21(8):846-53.
29. Shipitsin M, Campbell LL, Argani P, Weremowicz S, Bloushtain-Qimron N, Yao J, et al. Molecular definition of breast tumor heterogeneity. *Cancer Cell*. 2007 Mar;11(3):259-73.
30. Junttila MR, de Sauvage FJ. Influence of tumour micro-environment heterogeneity on therapeutic response. *Nature*. 2013 Sep 19;501(7467):346-54.
31. Simpson-Herren L, Noker PE, Wagoner SD. Variability of tumor response to chemotherapy. II. Contribution of tumor heterogeneity. *Cancer Chemother Pharmacol*. 1988;22(2):131-6.
32. Gatenby RA, Silva AS, Gillies RJ, Frieden BR. Adaptive therapy. *Cancer Res*. 2009 Jun 1;69(11):4894-903.
33. Eklund A, Nichols TE, Knutsson H. Cluster failure: Why fMRI inferences for spatial extent have inflated false-positive rates. *Proc Natl Acad Sci U S A*. 2016 Jul 12;113(28):7900-5.
34. Pham DL, Xu C, Prince JL. Current methods in medical image segmentation. *Annu Rev Biomed Eng*. 2000;2:315-37.
35. Padhani AR, Miles KA. Multiparametric imaging of tumor response to therapy. *Radiology*. 2010 Aug;256(2):348-64.
36. Vannier MW, Butterfield RL, Jordan D, Murphy WA, Levitt RG, Gado M. Multispectral analysis of magnetic resonance images. *Radiology*. 1985 Jan;154(1):221-4.
37. Asselin MC, O'Connor JP, Boellaard R, Thacker NA, Jackson A. Quantifying heterogeneity in human tumours using MRI and PET. *Eur J Cancer*. 2012 Mar;48(4):447-55.
38. Galban CJ, Chenevert TL, Meyer CR, Tsien C, Lawrence TS, Hamstra DA, et al. The parametric response map is an imaging biomarker for early cancer treatment outcome. *Nat Med*. 2009 May;15(5):572-6.
39. Mills SJ, Soh C, O'Connor JP, Rose CJ, Buonaccorsi G, Cheung S, et al. Enhancing fraction in glioma and its relationship to the tumoral vascular microenvironment: A dynamic contrast-enhanced MR imaging study. *AJNR Am J Neuroradiol*. 2010 Apr;31(4):726-31.
40. O'Connor JP, Carano RA, Clamp AR, Ross J, Ho CC, Jackson A, et al. Quantifying antivascular effects of monoclonal antibodies to vascular endothelial growth factor: insights from imaging. *Clin Cancer Res*. 2009 Nov 1;15(21):6674-82.
41. O'Connor JP, Jayson GC, Jackson A, Ghiorghiu D, Carrington BM, Rose CJ, et al. Enhancing Fraction Predicts Clinical Outcome following First-Line Chemotherapy in Patients with Epithelial Ovarian Carcinoma. *Clin Cancer Res*. 2007 Oct 15;13(20):6130-5.
42. Gaustad JV, Benjaminsen IC, Graff BA, Brurberg KG, Ruud EB, Rofstad EK. Intratumor heterogeneity in blood perfusion in orthotopic human melanoma xenografts assessed by dynamic contrast-enhanced magnetic resonance imaging. *J Magn Reson Imaging*. 2005 Jun;21(6):792-800.

43. Checkley D, Tessier JJ, Kendrew J, Waterton JC, Wedge SR. Use of dynamic contrast-enhanced MRI to evaluate acute treatment with ZD6474, a VEGF signalling inhibitor, in PC-3 prostate tumours. *Br J Cancer*. 2003 Nov 17;89(10):1889-95.
44. Brown JM, Wilson WR. Exploiting tumour hypoxia in cancer treatment. *Nat Rev Cancer*. 2004 Jun;4(6):437-47.
45. Even AJ, van der Stoep J, Zegers CM, Reymen B, Troost EG, Lambin P, et al. PET-based dose painting in non-small cell lung cancer: Comparing uniform dose escalation with boosting hypoxic and metabolically active sub-volumes. *Radiother Oncol*. 2015 Aug;116(2):281-6.
46. Gray LH, Conger AD, Ebert M, Hornsey S, Scott OC. The concentration of oxygen dissolved in tissues at the time of irradiation as a factor in radiotherapy. *Br J Radiol*. 1953 Dec;26(312):638-48.
47. Aerts HJ, van Baardwijk AA, Petit SF, Offermann C, Loon J, Houben R, et al. Identification of residual metabolic-active areas within individual NSCLC tumours using a pre-radiotherapy (18)Fluorodeoxyglucose-PET-CT scan. *Radiother Oncol*. 2009 Jun;91(3):386-92.
48. van Elmpt W, Zegers CM, Reymen B, Even AJ, Dingemans AM, Oellers M, et al. Multiparametric imaging of patient and tumour heterogeneity in non-small-cell lung cancer: quantification of tumour hypoxia, metabolism and perfusion. *Eur J Nucl Med Mol Imaging*. 2016 Feb;43(2):240-8.
49. Buffa FM, Harris AL, West CM, Miller CJ. Large meta-analysis of multiple cancers reveals a common, compact and highly prognostic hypoxia metagene. *Br J Cancer*. 2010 Jan 19;102(2):428-35.
50. Schilsky RL. Personalized medicine in oncology: the future is now. *Nat Rev Drug Discov*. 2010 May;9(5):363-6.
51. Wilson WR, Hay MP. Targeting hypoxia in cancer therapy. *Nat Rev Cancer*. 2011 Jun;11(6):393-410.
52. Threshold Pharmaceuticals Announces Its Two Phase 3 Studies Evaluating Evofosfamide Did Not Meet Primary Endpoints
<http://investor.thresholdpharm.com/releasedetail.cfm?ReleaseID=945765> (Accessed 25th August 2016).
53. Peeters SG, Zegers CM, Biemans R, Lieuwes NG, van Stiphout RG, Yaromina A, et al. TH-302 in Combination with Radiotherapy Enhances the Therapeutic Outcome and Is Associated with Pretreatment [18F]HX4 Hypoxia PET Imaging. *Clin Cancer Res*. 2015 Jul 1;21(13):2984-92.
54. Zips D, Zophel K, Abolmaali N, Perrin R, Abramyuk A, Haase R, et al. Exploratory prospective trial of hypoxia-specific PET imaging during radiochemotherapy in patients with locally advanced head-and-neck cancer. *Radiother Oncol*. 2012 Oct;105(1):21-8.
55. Tatum JL, Kelloff GJ, Gillies RJ, Arbeit JM, Brown JM, Chao KS, et al. Hypoxia: importance in tumor biology, noninvasive measurement by imaging, and value of its measurement in the management of cancer therapy. *Int J Radiat Biol*. 2006 Oct;82(10):699-757.
56. Dewhirst MW, Brier SR. Oxygen-Enhanced MRI Is a Major Advance in Tumor Hypoxia Imaging. *Cancer Res*. 2016 Feb 2;76:769-72.
57. Carlin S, Humm JL. PET of hypoxia: current and future perspectives. *J Nucl Med*. 2012 Aug;53(8):1171-4.
58. Peeters SG, Zegers CM, Lieuwes NG, van Elmpt W, Eriksson J, van Dongen GA, et al. A comparative study of the hypoxia PET tracers [(1)(8)F]HX4, [(1)(8)F]FAZA, and [(1)(8)F]FMISO in a preclinical tumor model. *Int J Radiat Oncol Biol Phys*. 2015 Feb 1;91(2):351-9.
59. Zegers CM, van Elmpt W, Szardenings K, Kolb H, Waxman A, Subramaniam RM, et al. Repeatability of hypoxia PET imaging using [(1)(8)F]HX4 in lung and head and neck cancer patients: a prospective multicenter trial. *Eur J Nucl Med Mol Imaging*. 2015 Nov;42(12):1840-9.

60. Nehmeh SA, Lee NY, Schroder H, Squire O, Zanzonico PB, Erdi YE, et al. Reproducibility of intratumor distribution of (18)F-fluoromisonidazole in head and neck cancer. *Int J Radiat Oncol Biol Phys*. 2008 Jan 1;70(1):235-42.
61. Zschaek S, Haase R, Abolmaali N, Perrin R, Stutzer K, Appold S, et al. Spatial distribution of FMISO in head and neck squamous cell carcinomas during radio-chemotherapy and its correlation to pattern of failure. *Acta Oncol*. 2015;54(9):1355-63.
62. Griffiths JR, Taylor NJ, Howe FA, Saunders MI, Robinson SP, Hoskin PJ, et al. The response of human tumors to carbogen breathing, monitored by Gradient-Recalled Echo Magnetic Resonance Imaging. *Int J Radiat Oncol Biol Phys*. 1997 Oct 1;39(3):697-701.
63. Halle C, Andersen E, Lando M, Aarnes EK, Hasvold G, Holden M, et al. Hypoxia-induced gene expression in chemoradioresistant cervical cancer revealed by dynamic contrast-enhanced MRI. *Cancer Res*. 2012 Oct 15;72(20):5285-95.
64. Hammond EM, Asselin MC, Forster D, O'Connor JP, Senra JM, Williams KJ. The meaning, measurement and modification of hypoxia in the laboratory and the clinic. *Clin Oncol (R Coll Radiol)*. 2014 May;26(5):277-88.
65. Linnik IV, Scott ML, Holliday KF, Woodhouse N, Waterton JC, O'Connor JP, et al. Noninvasive tumor hypoxia measurement using magnetic resonance imaging in murine U87 glioma xenografts and in patients with glioblastoma. *Magn Reson Med*. 2014 May;71(5):1854-62.
66. O'Connor JPB, Boulton JKR, Jamin Y, Babur M, Finegan KG, Williams KJ, et al. Oxygen-enhanced MRI accurately identifies, quantifies, and maps tumor hypoxia in preclinical cancer models. *Cancer Res*. 2016;76:787-95.
67. Remmele S, Sprinkart AM, Muller A, Traber F, von Lehe M, Gieseke J, et al. Dynamic and simultaneous MR measurement of R1 and R2* changes during respiratory challenges for the assessment of blood and tissue oxygenation. *Magn Reson Med*. 2013 Jul;70(1):136-46.
68. O'Connor JP, Naish JH, Parker GJ, Waterton JC, Watson Y, Jayson GC, et al. Preliminary study of oxygen-enhanced longitudinal relaxation in MRI: a potential novel biomarker of oxygenation changes in solid tumors. *Int J Radiat Oncol Biol Phys*. 2009 Nov 15;75(4):1209-15.
69. White DA, Zhang Z, Li L, Gerberich J, Stojadinovic S, Peschke P, et al. Developing oxygen-enhanced magnetic resonance imaging as a prognostic biomarker of radiation response. *Cancer Lett*. 2016 Sep 28;380(1):69-77.
70. Pettersson A, Graff RE, Ursin G, Santos Silva ID, McCormack V, Baglietto L, et al. Mammographic density phenotypes and risk of breast cancer: a meta-analysis. *J Natl Cancer Inst*. 2014 May;106(5).
71. Haralick RM, Shanmuga K, Dinstein I. Textural features for image classification. *IEEE Trans Systems Man Cybernetics*. 1973;6:610-21.
72. Peitgen H-O, Jurgens H, Saupe D. *Chaos and fractals*. Berlin: Springer; 2004.
73. Rose CJ, Mills SJ, O'Connor JP, Buonaccorsi GA, Roberts C, Watson Y, et al. Quantifying spatial heterogeneity in dynamic contrast-enhanced MRI parameter maps. *Magn Reson Med*. 2009 Aug;62(2):488-99.
74. Micheel C, Nass SJ, Omenn GS, Institute of Medicine Committee on the Review of Omics-Based Tests for Predicting Patient Outcomes in Clinical Trials. *Evolution of translational omics: lessons learned and the path forward*. Washington: National Academy of Sciences; 2012.
75. Sung NS, Crowley WF, Jr., Genel M, Salber P, Sandy L, Sherwood LM, et al. Central challenges facing the national clinical research enterprise. *Jama*. 2003 Mar 12;289(10):1278-87.
76. Cooksey D. *A review of UK health research funding*. Norwich: TSO; 2006.
77. Davnall F, Yip CS, Ljungqvist G, Selmi M, Ng F, Sanghera B, et al. Assessment of tumor heterogeneity: an emerging imaging tool for clinical practice? *Insights into imaging*. 2012 Dec;3(6):573-89.

78. Goh V, Sanghera B, Wellsted DM, Sundin J, Halligan S. Assessment of the spatial pattern of colorectal tumour perfusion estimated at perfusion CT using two-dimensional fractal analysis. *Eur Radiol.* 2009 Jun;19(6):1358-65.
79. Kido S, Kuriyama K, Higashiyama M, Kasugai T, Kuroda C. Fractal analysis of internal and peripheral textures of small peripheral bronchogenic carcinomas in thin-section computed tomography: comparison of bronchioloalveolar cell carcinomas with nonbronchioloalveolar cell carcinomas. *J Comput Assist Tomogr.* 2003 Jan-Feb;27(1):56-61.
80. Skogen K, Ganeshan B, Good C, Critchley G, Miles K. Measurements of heterogeneity in gliomas on computed tomography relationship to tumour grade. *J Neurooncol.* 2013 Jan;111(2):213-9.
81. Goh V, Ganeshan B, Nathan P, Juttla JK, Vinayan A, Miles KA. Assessment of response to tyrosine kinase inhibitors in metastatic renal cell cancer: CT texture as a predictive biomarker. *Radiology.* 2011 Oct;261(1):165-71.
82. Ganeshan B, Panayiotou E, Burnand K, Dizdarevic S, Miles K. Tumour heterogeneity in non-small cell lung carcinoma assessed by CT texture analysis: a potential marker of survival. *Eur Radiol.* 2012 Apr;22(4):796-802.
83. FDA.
<http://www.accessdata.fda.gov/scripts/cdrh/cfdocs/cfPMN/pmn.cfm?ID=K152186> (accessed 22nd August 2016).
84. O'Connor JP, Rose CJ, Jackson A, Watson Y, Cheung S, Maders F, et al. DCE-MRI biomarkers of tumour heterogeneity predict CRC liver metastasis shrinkage following bevacizumab and FOLFOX-6. *Br J Cancer.* 2011 Jun 28;105(1):139-45.
85. Kuo MD, Jamshidi N. Behind the numbers: Decoding molecular phenotypes with radiogenomics--guiding principles and technical considerations. *Radiology.* 2014 Feb;270(2):320-5.
86. Aerts HJ. The Potential of Radiomic-Based Phenotyping in Precision Medicine: A Review. *JAMA oncology.* 2016 Aug 18.
87. Aerts HJ, Velazquez ER, Leijenaar RT, Parmar C, Grossmann P, Cavalho S, et al. Decoding tumour phenotype by noninvasive imaging using a quantitative radiomics approach. *Nature communications.* 2014;5:4006.
88. Kumar V, Gu Y, Basu S, Berglund A, Eschrich SA, Schabath MB, et al. Radiomics: the process and the challenges. *Magn Reson Imaging.* 2012 Nov;30(9):1234-48.
89. Coroller TP, Grossmann P, Hou Y, Rios Velazquez E, Leijenaar RT, Hermann G, et al. CT-based radiomic signature predicts distant metastasis in lung adenocarcinoma. *Radiother Oncol.* 2015 Mar;114(3):345-50.
90. Wu W, Parmar C, Grossmann P, Quackenbush J, Lambin P, Bussink J, et al. Exploratory Study to Identify Radiomics Classifiers for Lung Cancer Histology. *Frontiers in oncology.* 2016;6:71.
91. Segal E, Sirlin CB, Ooi C, Adler AS, Gollub J, Chen X, et al. Decoding global gene expression programs in liver cancer by noninvasive imaging. *Nature biotechnology.* 2007 Jun;25(6):675-80.
92. Zhu Y, Li H, Guo W, Drukker K, Lan L, Giger ML, et al. Deciphering Genomic Underpinnings of Quantitative MRI-based Radiomic Phenotypes of Invasive Breast Carcinoma. *Scientific reports.* 2015;5:17787.
93. Just N. Improving tumour heterogeneity MRI assessment with histograms. *Br J Cancer.* 2014 Sep 30.
94. Issa B, Buckley DL, Turnbull LW. Heterogeneity analysis of Gd-DTPA uptake: improvement in breast lesion differentiation. *J Comput Assist Tomogr.* 1999 Jul-Aug;23(4):615-21.
95. Gillies RJ, Anderson AR, Gatenby RA, Morse DL. The biology underlying molecular imaging in oncology: from genome to anatome and back again. *Clin Radiol.* 2010 Jul;65(7):517-21.
96. Yang X, Knopp MV. Quantifying tumor vascular heterogeneity with dynamic contrast-enhanced magnetic resonance imaging: a review. *Journal of biomedicine & biotechnology.* 2011;2011:732848.

97. Poste G. Bring on the biomarkers. *Nature*. 2011 Jan 13;469(7329):156-7.
98. Hayes DF, Allen J, Compton C, Gustavsen G, Leonard DG, McCormack R, et al. Breaking a vicious cycle. *Science translational medicine*. 2013 Jul 31;5(196):196cm6.
99. ISO. 3534-2:2006 Statistics – Vocabulary and symbols – Part 2: Applied statistics (accessed 30th November 2015).
100. Sullivan DC, Obuchowski NA, Kessler LG, Raunig DL, Gatsonis C, Huang EP, et al. Metrology Standards for Quantitative Imaging Biomarkers. *Radiology*. 2015 Dec;277(3):813-25.
101. Aerts HJ, Bussink J, Oyen WJ, van Elmpt W, Folgering AM, Emans D, et al. Identification of residual metabolic-active areas within NSCLC tumours using a pre-radiotherapy FDG-PET-CT scan: a prospective validation. *Lung Cancer*. 2012 Jan;75(1):73-6.
102. Carano RA, Ross AL, Ross J, Williams SP, Koeppen H, Schwall RH, et al. Quantification of tumor tissue populations by multispectral analysis. *Magn Reson Med*. 2004 Mar;51(3):542-51.
103. Henning EC, Azuma C, Sotak CH, Helmer KG. Multispectral quantification of tissue types in a RIF-1 tumor model with histological validation. Part I. *Magn Reson Med*. 2007 Mar;57(3):501-12.
104. Chen L, Choyke PL, Chan TH, Chi CY, Wang G, Wang Y. Tissue-specific compartmental analysis for dynamic contrast-enhanced MR imaging of complex tumors. *IEEE Trans Med Imaging*. 2011 Dec;30(12):2044-58.

FIGURES

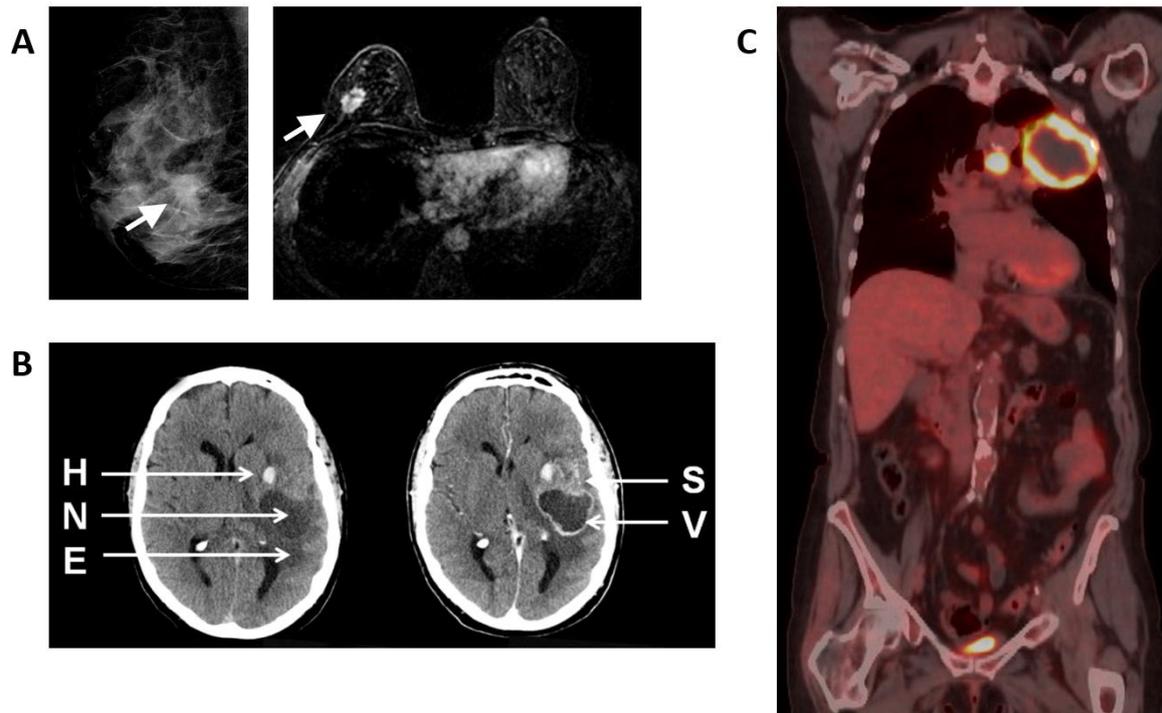


Figure 1

Examples of measuring heterogeneity in routine clinical practice: A, lesion spiculation is a feature of the BI-RADS categorization used in assessment of likelihood of breast lesions being malignant. Here a spiculated cancer is shown on x-ray mammography and on MRI scan (indicated by white arrows). B, spatial variation in haemorrhage (H), necrosis (N), peri-lesion edema (E), vascular enhancement (V) and solid tumor (S) are frequently described in radiological reports such as for this high grade glioma and can influence how tumor volume is calculated in neuro-radiological practice. C, spatial variation underpins the notion of reporting a maximum value of standardized uptake value in ^{18}F FDG-PET CT, such as is the left apical non-small cell lung cancer with central necrosis and peripheral highly metabolically active tumor.

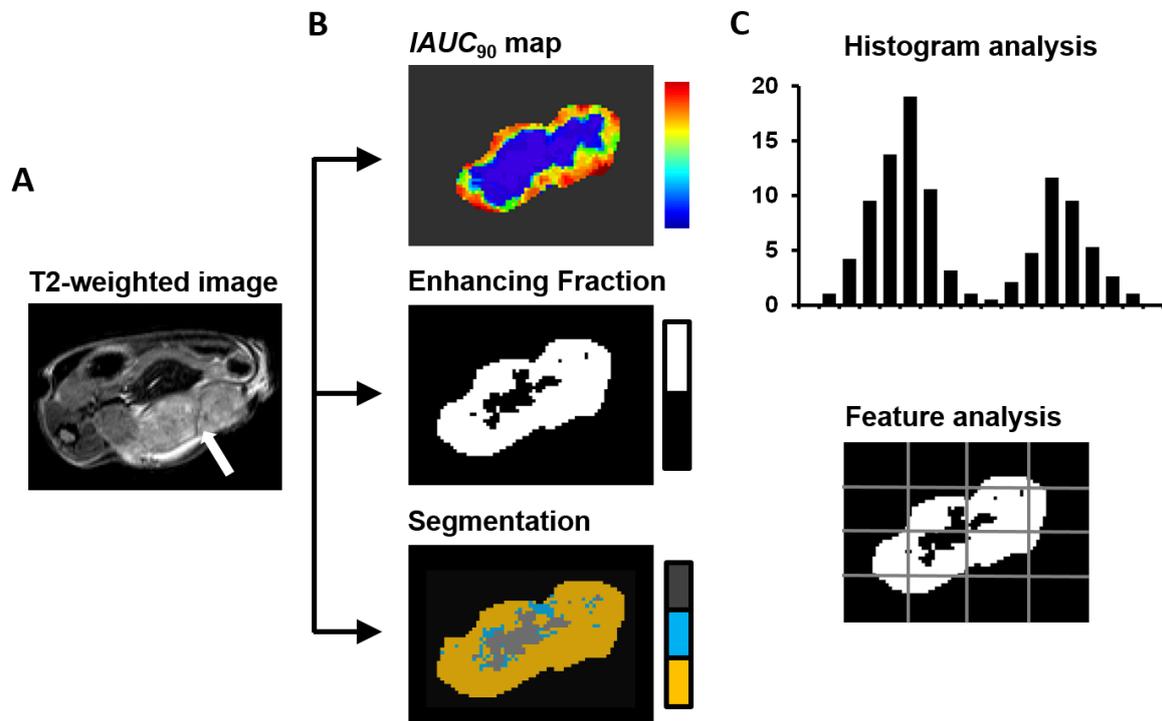


Figure 2

Methods for quantifying intratumoral heterogeneity: A, an example 786-0 renal cancer xenograft tumor is shown on a T2-weighted anatomical image. B, tumor function is assessed by DCE-MRI (top) and the same data can be binarized to define enhancing tumor (middle) before combined with other MRI signals to produce a segmented image (bottom). C, the data can also be treated as a distribution for histogram analysis (top) or can be subject to a feature analysis, such as box counting.

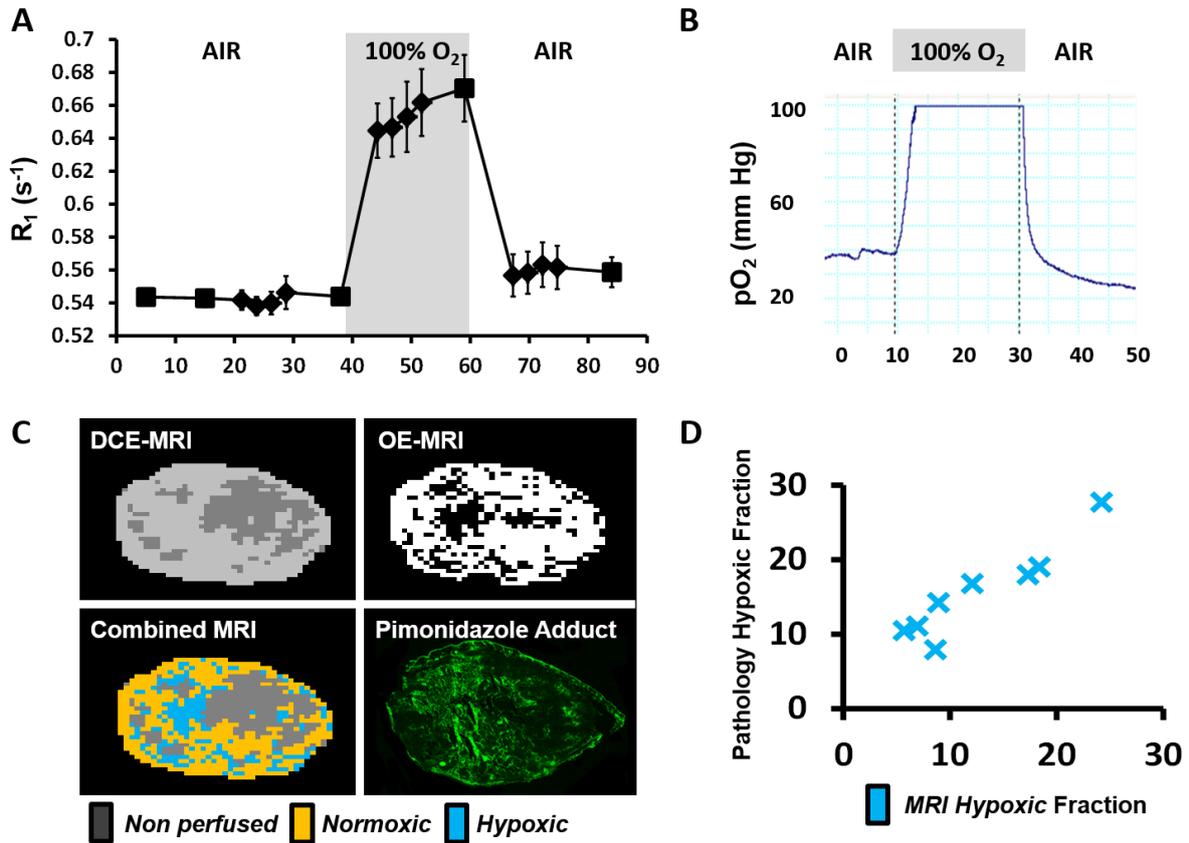
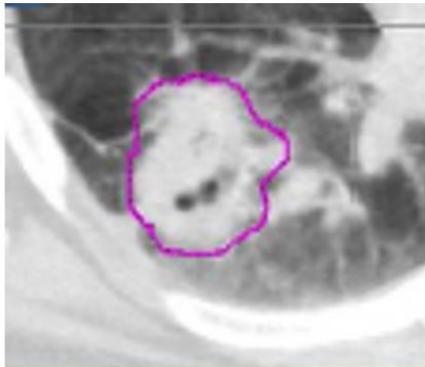


Figure 3

Imaging hypoxia with oxygen-enhanced MRI (OE-MRI): A, longitudinal relaxation rate (R_1) measured in preclinical xenografts models is stable when breathing air, but shows significant increase during oxygen inhalation. B, OE-MRI signal changes mirror the time course of change in tumor pO₂ detected by Oxylite measurement in the same xenografts (maximum to the detection range was 100 mmHg). C, DCE-MRI is used to identify perfused tumor and then OE-MRI maps are analyzed for hypoxic tumor, defined by lack of positive change with oxygen challenge. Representative MRI maps are shown in SW620 colorectal cancer xenografts, along with a segmentation that defines non-perfused, normoxic and hypoxic tumor sub-regions. Companion data is from Immunofluorescence-based assay of pimonidazole adduct formation. D, the hypoxic fraction defined by MRI closely correlates with the equivalent measurement defined by pathology, providing biological validation of the technique. Adapted from reference 66.

A

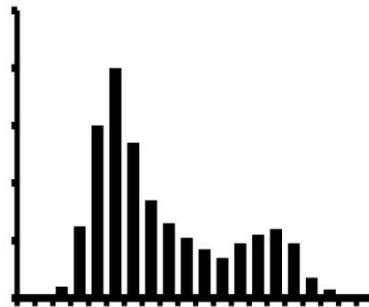
Quantitative imaging and tumor delineation



Lung cancer on CT scan

B

Segmentation and radiomic profiling



C

Data integration, validation and qualification

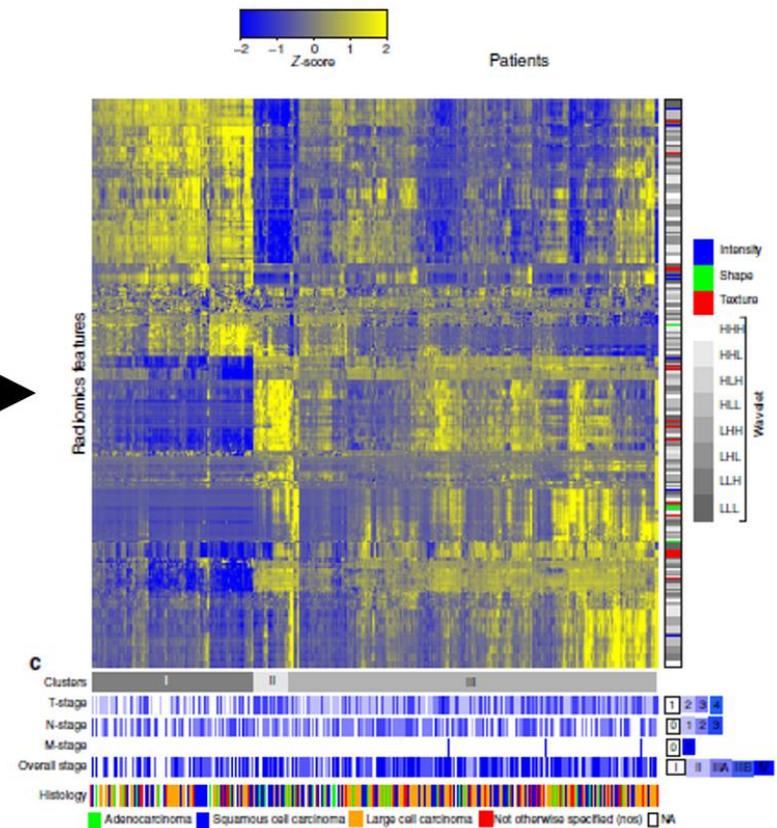


Figure 4

Radiomic analysis of tumor data: A, quantitative imaging is performed and the tumor is delineated, here in an example of a patient with lung cancer. B, segmentation and radiomic profiling are performed to identify many tens to hundreds of features based on semantic characteristics, texture analysis and histogram analysis. C, radiomic data is integrated with genomic and proteomic data along with clinical information to provide a signature, which is effectively a biomarker. The radiomic signature must then be validated and qualified for clinical use. Adapted from reference 87.

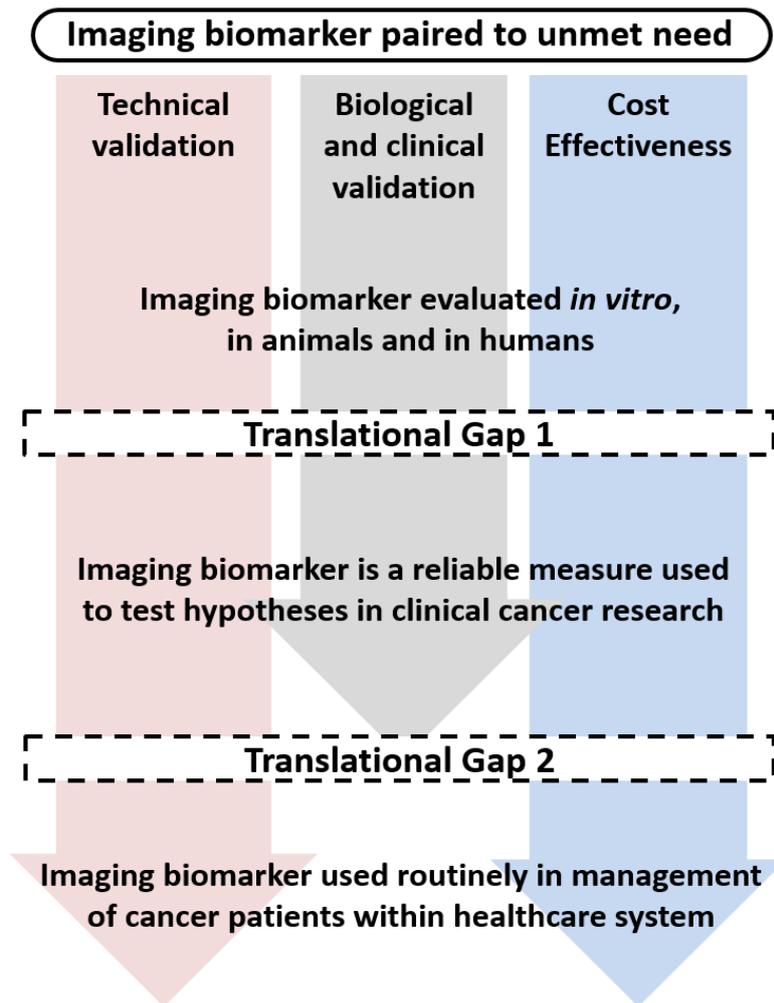


Figure 5

Roadmap for validating and qualifying imaging biomarkers: all imaging biomarkers must cross a translational gap from initial testing to become robust medical research tools. A second translational gap must be crossed for the imaging biomarker to become integrated into routine patient care. This achieved through three parallel tracks of technical validation, biological and clinical validation, and cost effectiveness, followed by qualification. Adapted from reference 18.